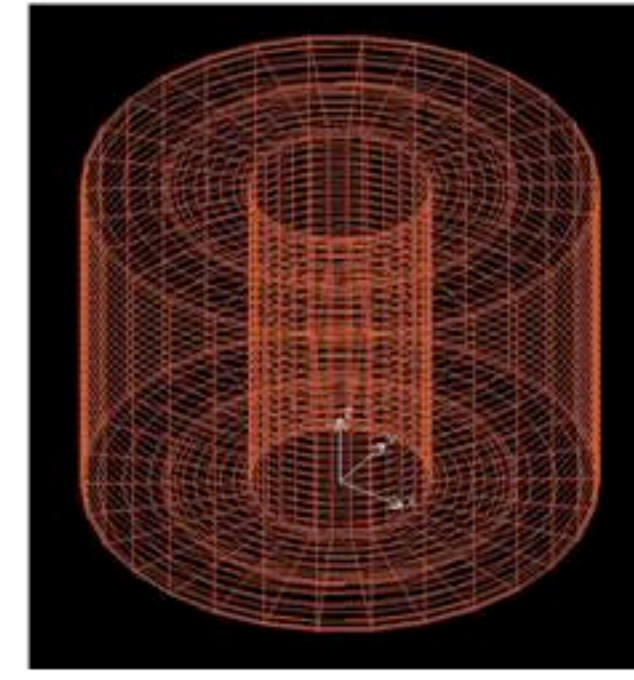


Dynamo Action in MRI-Driven Turbulence in a Cylindrical Annulus

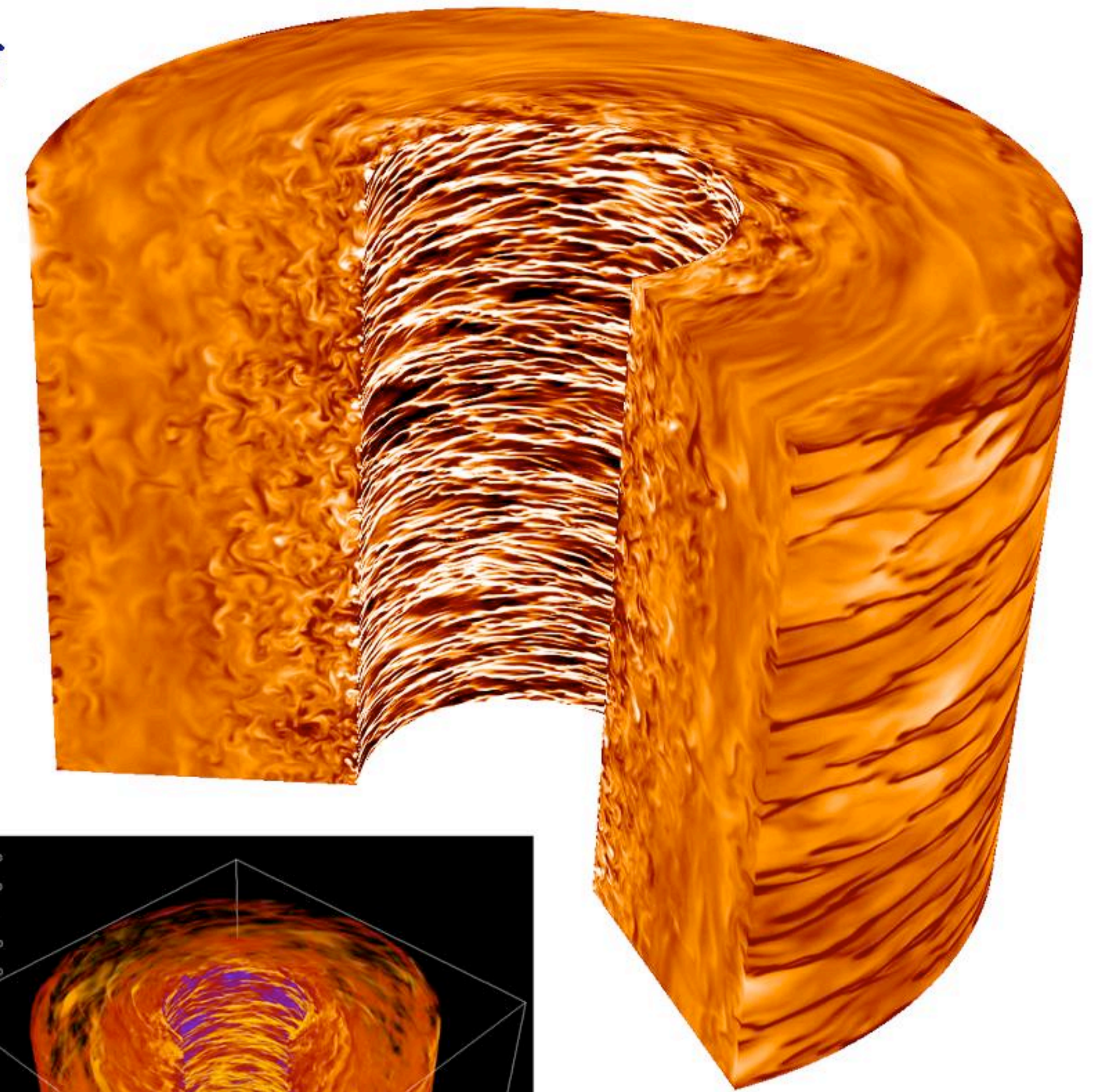
Aleksandr Obabko^{1,2}, Fausto Cattaneo^{1,2,3} and Paul Fischer^{3,4}

Axisymmetric and fully 3D global incompressible MHD numerical simulations of MRI-driven turbulence in cylindrical annulus with finite viscosity and resistivity:

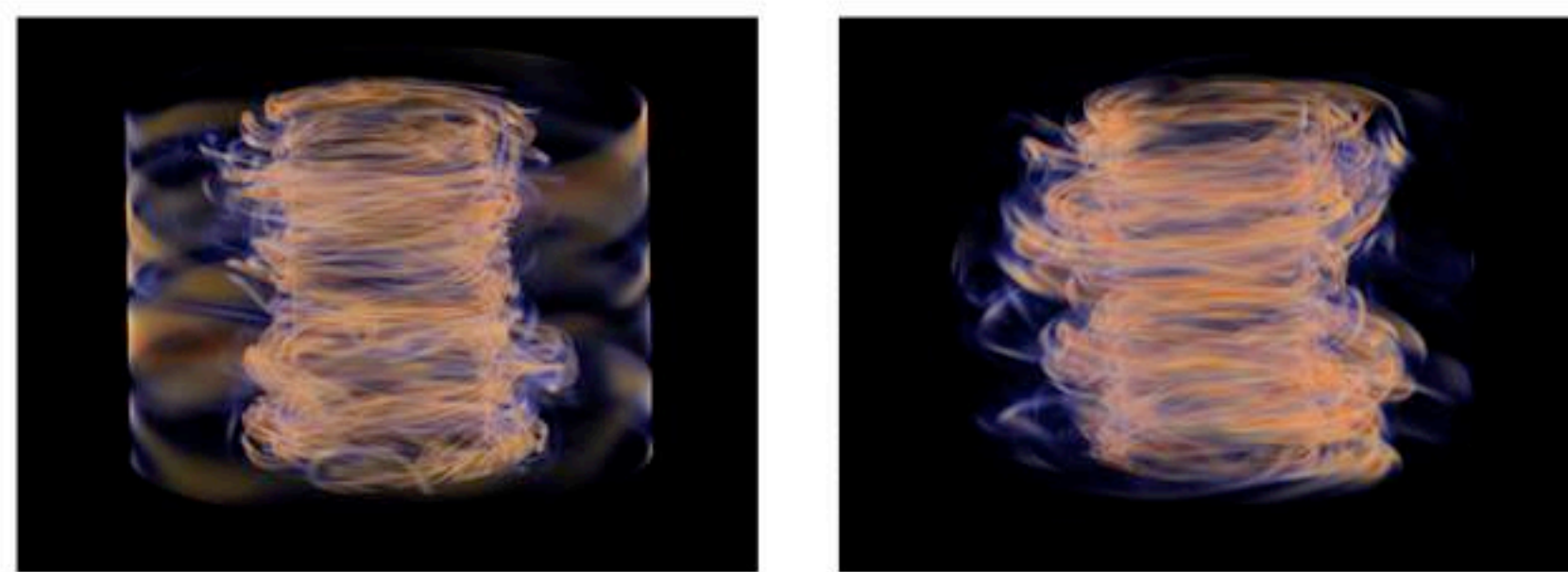
- ✓ upto $Re=62000$ and $Rm=31000$ ($Pm=0.5$)
- ✓ ANL spectral element code Nekton 5000 with upto 155000 elements and 10^3 collocation points per element^{5, 6, 7}
- ✓ in the geometry inspired by Princeton MRI liquid sodium experiment (Schartman, Burin, Goodman & Ji 2006; Obabko, Cattaneo & Fischer 2008)



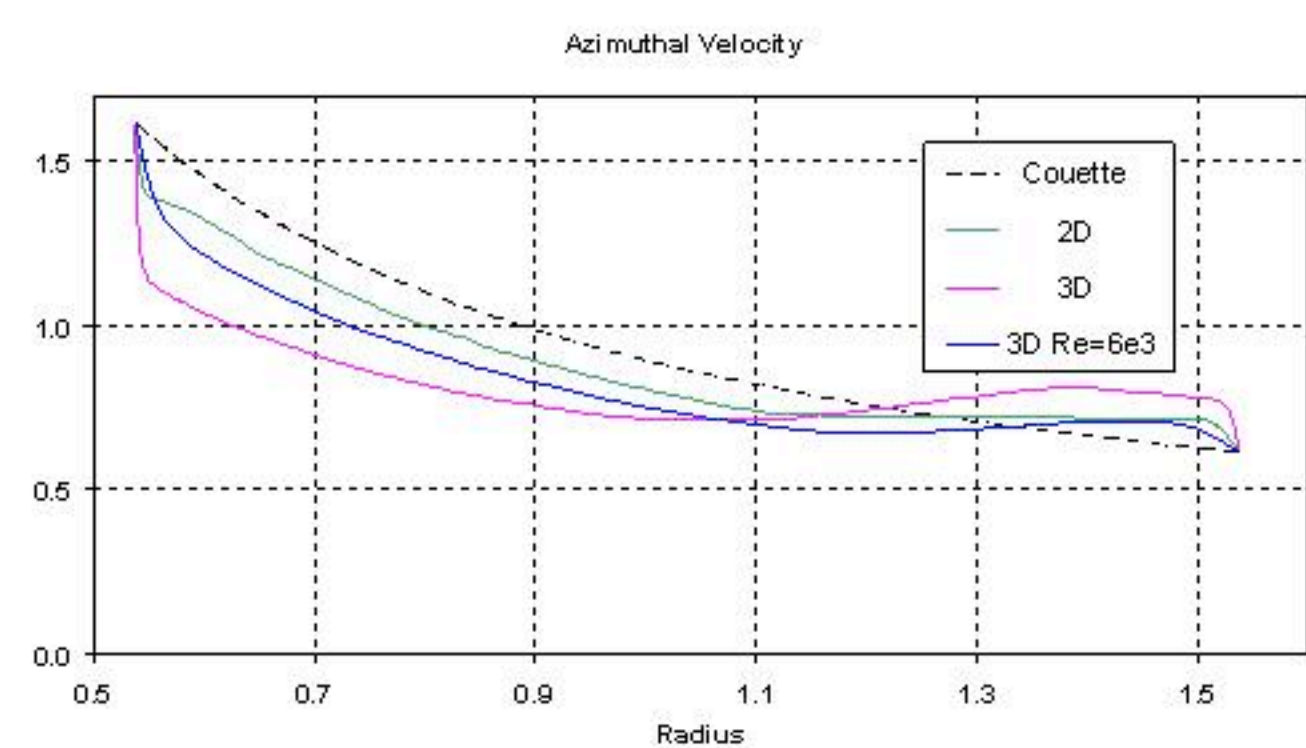
Nekton 5000 spectral element grid.



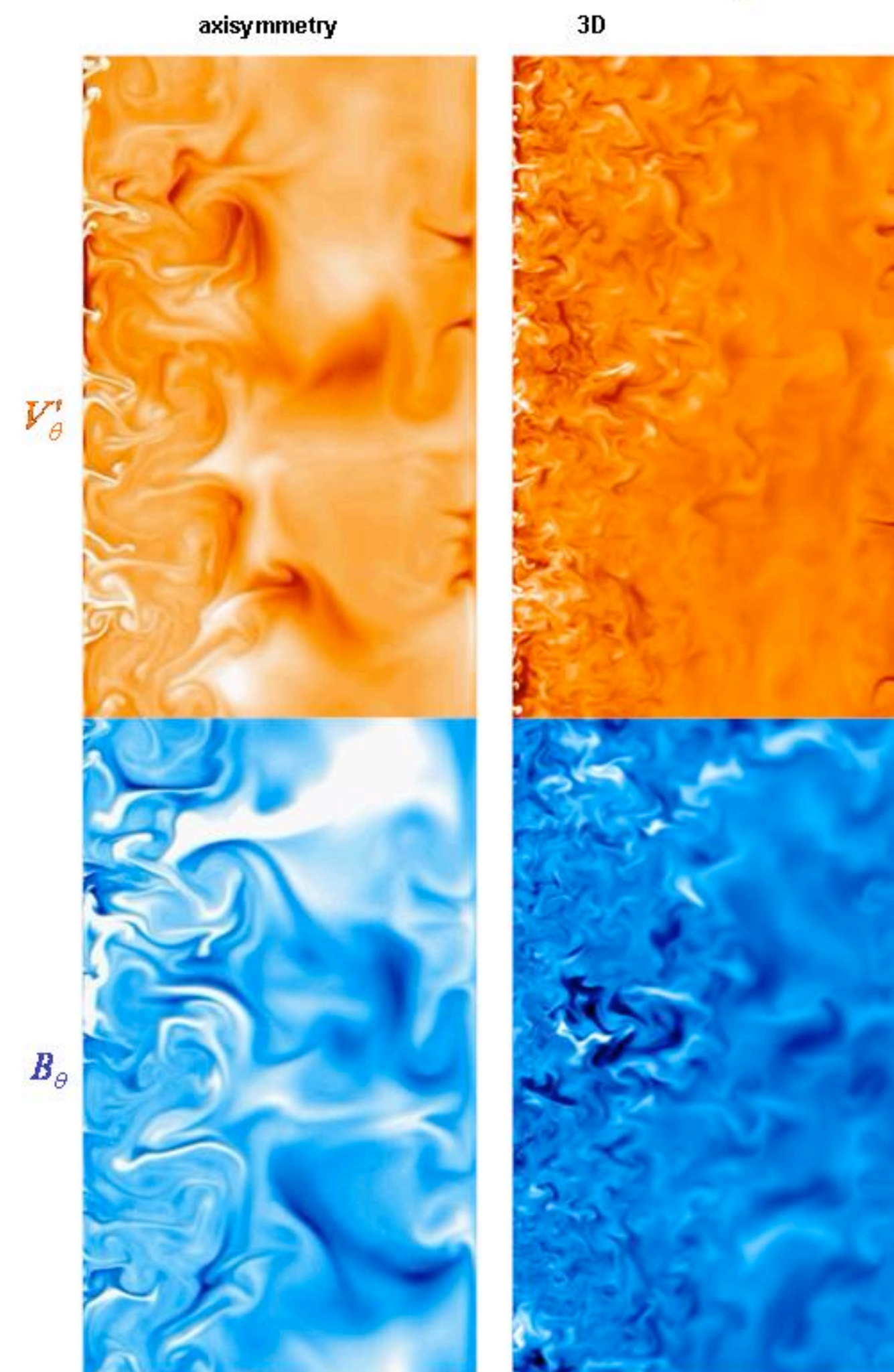
Pseudocolor plot (upper) and volume rendering (left⁸) of fluctuation of the azimuthal velocity field in 3D case with for $Re=62000$. The fluctuations in azimuthal velocity have a structure of spiraling eddies and of high (light) and low (dark) speed streaks near cylinder boundaries.



Viscous (left) and ohmic (right) dissipation⁸ in the non-linear saturation of MRI at $Re=6200$. The MRI saturation is achieved through comparable levels of viscous and ohmic dissipation.



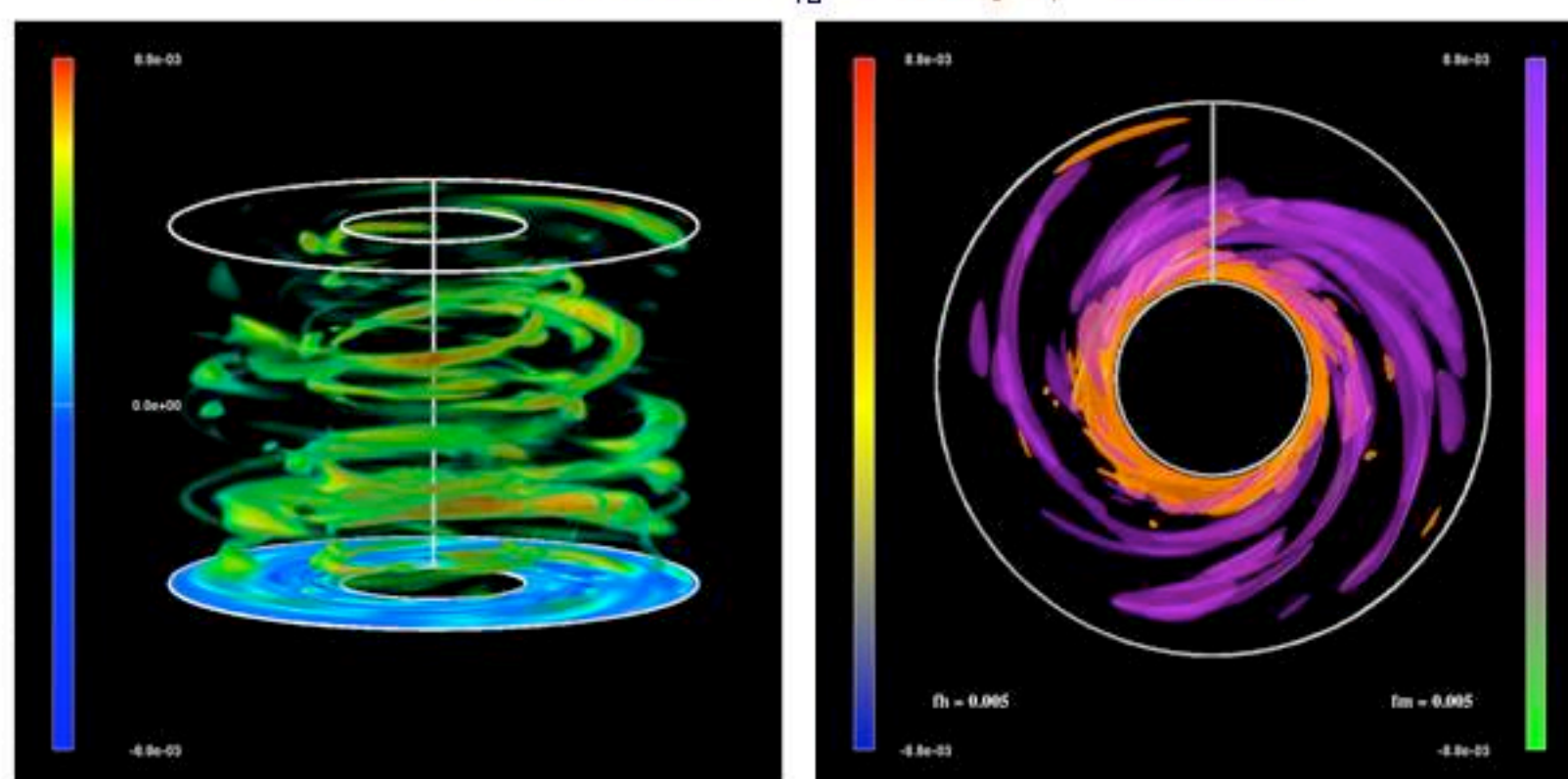
Averaged azimuthal velocity for axisymmetric case at $Re=62000$ (green) and 3D case at $Re=6200$ (blue) and $Re=62000$ (red). The MRI saturation also involves modification of background velocity toward solid body rotation in 3D but flat rotational profile in axisymmetry.



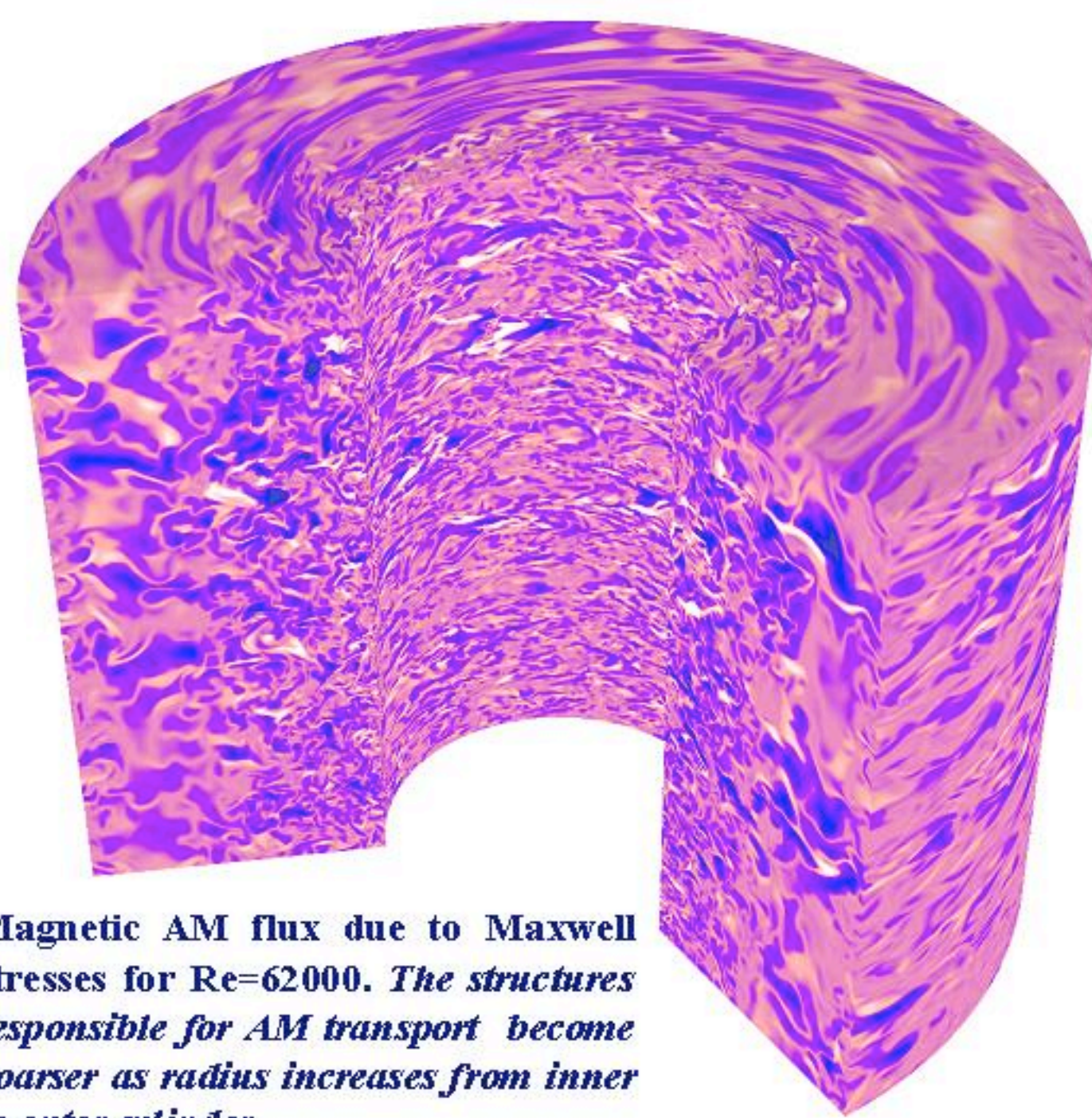
Poloidal cut of fluctuation of the azimuthal velocity (orange) and azimuthal magnetic field (blue) in axisymmetry (left) and in 3D (right) for $Re=62000$. The transition from finer to coarser structures in velocity and magnetic field with radius increasing from the inner (left vertical boundary) to the outer cylinder (right vertical boundary) occurs sharply in axisymmetry being more diffused in 3D.

Angular Momentum Transport

$$AM \text{ Flux } F_{Tz} = rV_\theta V_r - rB_\theta B_r$$

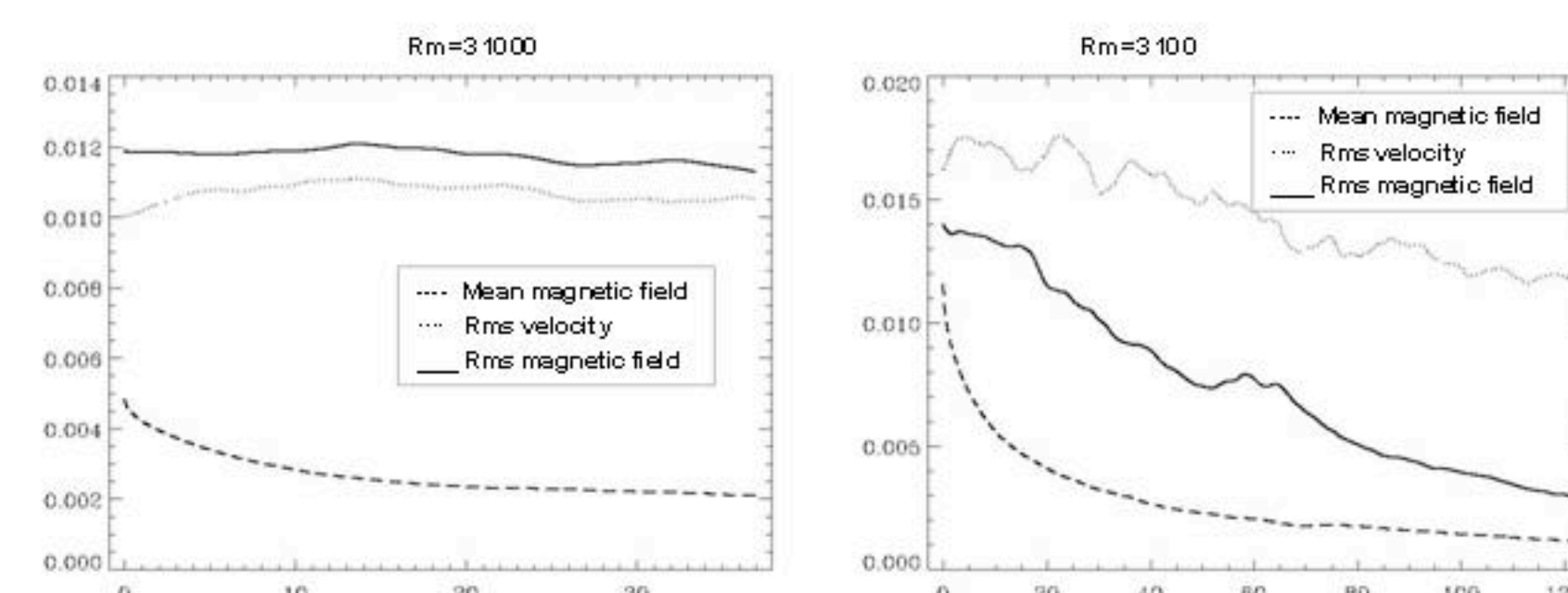


AM flux⁸ for $Re=6200$ on the left and its contributions due to the velocity fluctuations (orange) and magnetic field (violet) on the right. The Maxwell stresses dominate AM transport in the interior of the annulus while Reynolds stresses are important in cylinder boundary layers.

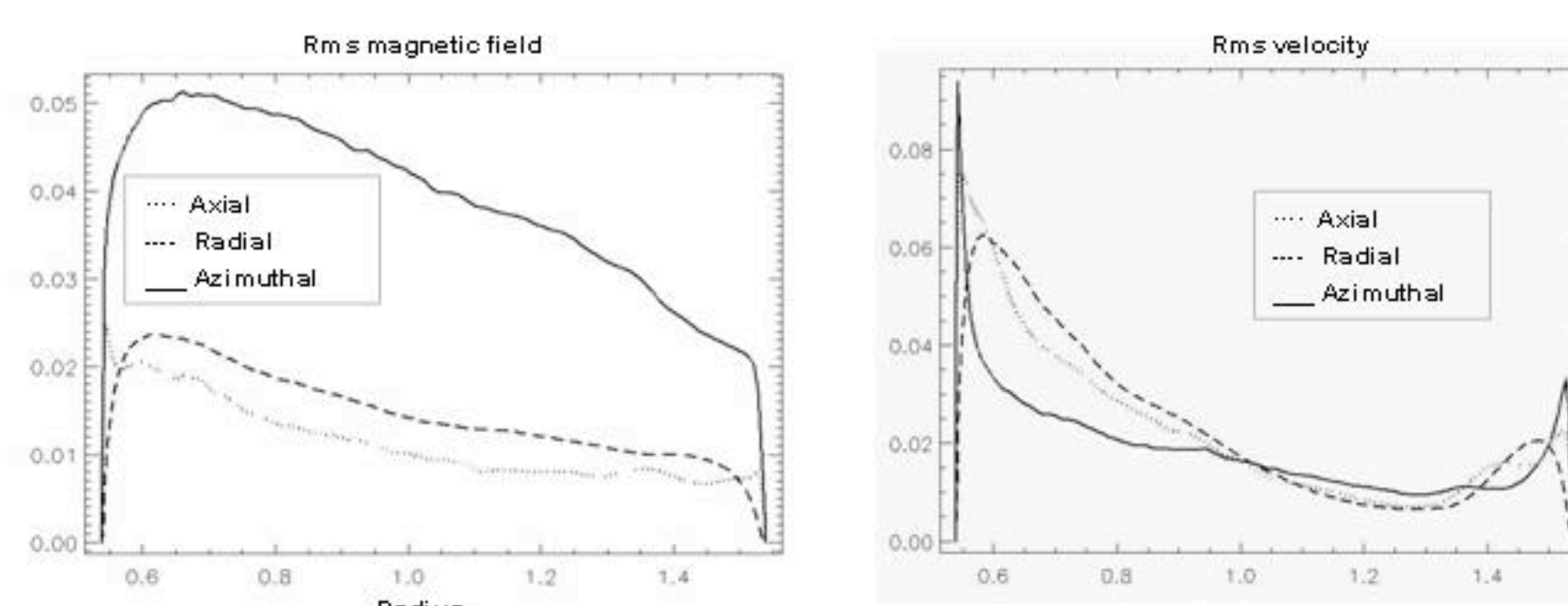


Magnetic AM flux due to Maxwell stresses for $Re=62000$. The structures responsible for AM transport become coarser as radius increases from inner to outer cylinder.

Small-Scale Dynamo at $Pm=0.5$



Time traces of volume-average of mean magnetic field (dashed) and of root-mean-square of magnetic field (solid) and velocity (dotted) for 3D case with $Pm=0.5$ and with $Rm=31000$ (left) and $Rm=3100$ (right) after switching off external magnetic field at the cylinder boundaries. The fluctuations of magnetic field survive a decay of the mean magnetic field at high enough Rm .



Cylinder-average of azimuthal (solid), radial (dashed) and axial (dotted) components of root-mean-square of magnetic field (left) and velocity (right) for 3D cases with $Pm=0.5$ and $Rm=31000$ ($Re=62000$). The fluctuations of magnetic field are about 50 times smaller than characteristic shear velocity (~ 1) leading to the local Rm (based on rms velocity and correlation length) of the order 10^2 which is typical of small-scale dynamo systems.

Conclusions :

- ✓ Nonlinear saturation of MRI:
 - comparable viscous and ohmic dissipation
 - modification of the base flow toward solid body rotation in 3D and flat rotational profile in axisymmetry
 - angular momentum transport is dominated by Maxwell stresses
- ✓ Small-scale dynamo at $Pm=0.5$:
 - fluctuation of magnetic field survive a decay of the mean magnetic field at high enough magnetic Reynolds number Rm
 - dynamo at magnetic Prandtl number below one
 - typical small-scale dynamo system with the local Rm of the order of a few hundreds

References:

- Ji H, Schartman E, Burin M & Goodman J. 2006. Nature 444, 343
Obabko A., Cattaneo F. & Fischer P. 2008. Physica Scripta, accepted

¹ CMSO, ² University of Chicago, ³ Argonne National Laboratory (ANL)

⁴ supported by the Office of Science of the US DOE under Contract No. W-31-109-Eng-38

⁵ used NERSC resources supported by the Office of Science of the US DOE under Contract No. DE-AC03-76SF00098 (INCITE 2005 award)

⁶ run time on 32768 processors of Blue Gene Watson (BGW) was provided courtesy of the IBM Corporation

⁷ acknowledge the use of 2048-processor IBM Blue Gene/L (BGL) system operated by the Argonne Leadership Computing Facility at ANL

⁸ acknowledge the help of Cristina Siegerist and Gunter Weber, NERSC Visualization Group, Lawrence Berkeley National Laboratory